Torsional buckling and post-buckling of columns made of aluminium alloy

Czesław Szymczak [a], Marcin Kujawa [b],[*]

[a] Faculty of Ocean Engineering and Ship Technology, Department of Structural Engineering, Gdańsk University of Technology, G. Narutowicza 11/12, 13, 80–233 Gdańsk, Poland
[b] Faculty of Civil and Environmental Engineering, Department of Structural Mechanics, Gdańsk University of Technology, G. Narutowicza 11/12, 13, 80–233 Gdańsk, Poland

ARTICLE INFO

ABSTRACT

The paper concerns torsional buckling and the initial post-buckling of axially compressed thin-walled aluminium alloy columns with bisymmetrical cross-section. It is assumed that the column material behaviour is described by the Ramberg–Osgood constitutive equation in non-linear elastic range. The stationary total energy principle is used to derive the governing non-linear differential equation. An approximate solution of the equation determined by means of the perturbation approach allows to determine the buckling loads and the initial post-buckling behaviour. Numerical examples dealing with simply supported I-column are presented and the effect of material elastic non-linearity on the critical loads and initial post-buckling behaviour are compared to the linear solution.

© 2018 Elsevier Inc. All rights reserved.

1. Introduction

The thin-walled members made of aluminium are increasingly found in various fields of engineering structures in the light of their strength relative to the weight [1–3]. As is well known under the influence of compression there are problems related to loss of stability: global (flexural, torsional, flexural-torsional), local and distortional modes depending on the parameters of the cross-section, the column length and the mechanical properties of the column material. The problems of different types of buckling, especially torsional buckling are well described in literature [4]. Recently special problems related to mainly flexural-torsional buckling are taken into consideration in analytical–numerical–experimental [5–8], experimental–numerical [9] or experimental [10,11] routines, using different materials (e.g. steel, aluminium, laminated structural glass, wood composite) but appropriate attention is paid neither to torsional buckling [12] nor post-buckling behaviour of columns [13]. Most of the papers focused on torsional buckling and post-buckling refer to cylindrical shells only [14,15] in linear or non-linear sense. A relatively comprehensive theoretical review (in mathematical view) of major problems for buckling and post-buckling of rods and shells in linear and non-linear elastic ranges can be found in a monograph by Antman [16]. Two articles written by Hancock are also worth mentioning [17,18]. In these articles the author reviews research on cold-formed structures conducted in recent years.

---

* Corresponding author.
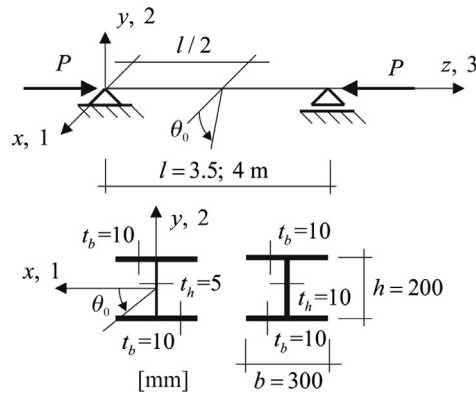 *E-mail address:* mark@pg.edu.pl (M. Kujawa).

Fig. 1. Axially compressed columns; numerical example – data.

In this paper torsional buckling and initial post-buckling behaviour of axially compressed column made of aluminium alloy [19] is analysed. The material behaviour is described by the Ramberg–Osgood law [20,21]. In order to find the analytical solution of the problem at first the total potential energy of the structure and applied loads is formulated based upon the classical theory of beams in initial finite displacements range [22]. The governing nonlinear differential equation is derived with the aid of the stationary total potential energy principle. The approximate solution of the equation obtained by means of a perturbation approach [22] leads to the critical buckling load and the initial post-buckling behaviour. The critical load follows the tangent modulus approach [23]. In order to verify the analytical results numerical examples dealing with I-columns are presented and comparison with the FEM results using ABAQUS software [24] is shown. A good agreement of both kind of stability analysis is achieved here.

2. Total potential energy of column and governing differential equation

Consider an axially compressed thin-walled column with bisymmetric cross-section (see Fig. 1) made of non-linear elastic material described by the Ramberg–Osgood relationship (1) [21]

$$\varepsilon = \frac{\sigma}{E} + K\left(\frac{\sigma}{\sigma_0}\right)^{n-1} \tag{1}$$

where σ is the axial stress, E stands for the Young's modulus, σ_0 denotes the yield stress, ε strain, K and n are material constants. It is well known that three independent global buckling modes are possible: two flexural about axes of symmetry and a torsional one. The tangent modulus theory [20] is adopted to find the torsional buckling load and initial post-bucking behaviour. The tangent modulus is determined by the first derivative of the constitutive Eq. (1) with respect to the strain ε

$$E_t = \frac{d\sigma}{d\varepsilon} = E\big[1 + (n-1)KE\sigma^{n-2}\sigma_0^{1-n}\big]^{-1} \tag{2}$$

Following [25] the critical buckling load P_{cr}^l corresponding to the linear elastic material is

$$P_{cr}^l = \frac{A}{J_0}\left[\frac{\pi^2 E J_\omega}{l_b^2} + G J_d\right] \tag{3}$$

where J_0 stands for the polar moment of inertia, J_ω is the cross-sectional warping moment of inertia, A is for the cross-section area, G represents the shear modulus, J_d is the free-torsion moment of inertia and l_b stands for the effective buckling length depending on the boundary conditions of the column. In order to find the critical buckling load in nonlinear elastic range of the column material behaviour the tangent modulus E_t (2) should be inserted instead the Young's modulus in (3) and after some algebra we arrive at the non-linear algebraic equation for the critical buckling load

$$P_{cr} + KEA(n-1)P_{cr}^{n-1}P_0^{1-n} = P_{cr}^l \tag{4}$$

where $P_0 = \sigma_0 A$. Herein it is assumed that the Poisson's ratio ν in non-linear range is independent of the strain ε and hence

$$G_t = \frac{E_t}{2(1+\nu)} \tag{5}$$

In the initial post-buckling state the axial stress σ_1 and the axial strain ε_1 due to the column torsion θ (see Fig. 1) may be written as

$$\sigma_1 = \sigma - \sigma_{cr}, \quad \varepsilon_1 = \varepsilon - \varepsilon_{cr} \tag{6}$$

where the critical buckling stress denoted by σ_{cr} may be determined using solution of the Eq. (4)

$$\sigma_{cr} = \frac{P_{cr}}{A} \tag{7}$$

and the critical buckling strain ε_{cr} can be computed from the relation (1).

Expansion of the relation $\sigma_1(\varepsilon_1)$ in the vicinity of the bifurcation point $(\sigma_{cr}, \varepsilon_{cr})$ into Taylor series leads to

$$\sigma_1 = E_t \varepsilon_1 + E_1 \varepsilon_1^2 + E_2 \varepsilon_1^3 + \cdots \tag{8}$$

where E_1 and E_2 are regarded as the second and the third moduli expressed by corresponding stress σ_1 derivatives with respect to the strain ε_1 at the bifurcation point $(\sigma_{cr}, \varepsilon_{cr})$

$$E_1 = \frac{1}{2} \frac{d^2\sigma_1}{d\varepsilon_1^2}(\sigma_{cr}, \varepsilon_{cr}), E_2 = \frac{1}{6} \frac{d^3\sigma_1}{d\varepsilon_1^3}(\sigma_{cr}, \varepsilon_{cr}) \tag{9}$$

The close analytical formulas for these derivatives are derived by means of successive differentiation of the relationship (1)

$$\frac{d^2\sigma_1}{d\varepsilon_1^2} = -\frac{KE(n-1)(n-2)}{1 + K(n-1)\left(\frac{\sigma_{cr}}{\sigma_0}\right)^{n-1}\left(\frac{E}{\sigma_{cr}}\right)}\left(\frac{\sigma_{cr}}{\sigma_0}\right)^{n-3}\left(\frac{E_t}{\sigma_0}\right)^2$$

$$\frac{d^3\sigma_1}{d\varepsilon_1^3} = -\frac{KE(n-1)(n-2)}{1 + K(n-1)\left(\frac{\sigma_{cr}}{\sigma_0}\right)^{n-1}\left(\frac{E}{\sigma_{cr}}\right)}\left(\frac{E_t}{\sigma_{cr}}\right)\left(\frac{E_1}{\sigma_{cr}}\right)\left(\frac{\sigma_{cr}}{\sigma_0}\right)^{n-1}\cdots \tag{10}$$

$$\cdots\left[6 + (n-3)\left(\frac{E_t}{\sigma_{cr}}\right)\left(\frac{E_t}{E_1}\right)\right]$$

The total potential energy of the column V in the initial post-buckling state consists of the strain energy V_S and the potential energy of the applied end loads V_P

$$V = V_S + V_P \tag{11}$$

The strain energy is a sum of the effect of the normal stress V_σ the energy due to free torsion V_t

$$V_S = V_\sigma + V_t \tag{12}$$

where the first part may be written as the integral on the column volume W

$$V_S = \int_W \int_0^{\sigma_1} \sigma_1 d\varepsilon_1 dW \tag{13}$$

and the second one [4,25]

$$V_t = \frac{1}{2} G_t J_d \int_0^l \theta'^2 dz \tag{14}$$

where l is the column length, θ is the torsion angle, the prime denotes derivative with respect to z.

In order to calculate the integral (13) a well-known relation for the axial strain due to the column torsion is applied [25]

$$\varepsilon_1 = \omega\theta'' + \frac{1}{2}\left(r^2 - \frac{J_0}{A}\right)\theta'^2 \tag{15}$$

where ω is the sectorial area and r denotes the polar coordinate of cross-section point.

Inserting the relation (8) into the integral (13) and neglecting the terms higher than third order we arrive at

$$V_S = \int_0^l \int_A \left(\frac{1}{2}E_t\varepsilon_1 + \frac{1}{3}E_1\varepsilon_1^2 + \frac{1}{4}E_2\varepsilon_1^3\right) dA dz \tag{16}$$

Using (15) and integrating on whole cross-section the integral (16) may be rewritten as

$$V_S = \frac{1}{2}E_t J_\omega \int_0^l \theta''^2 dz + \frac{1}{8}E_t \bar{J}_{00} \int_0^l \theta'^2 dz + \frac{1}{4}E_2 J_{\omega\omega} \int_0^l \theta''^4 dz \tag{17}$$

where the terms higher than fourth order of derivatives of the torsion of angle are neglected. The following notations are introduced:

- the warping torsional moment of inertia $J_\omega = \int_A \omega^2 dA$,
- the fourth order polar moment of inertia $J_{00} = \int_A r^4 dA$,
- the reduced fourth order polar moment of inertia $\bar{J}_{00} = J_{00} - \frac{J_0^2}{A}$,
- the fourth order warping moment of inertia $J_{\omega\omega} = \int_A \omega^4 dA$.

The potential energy of axial end loads P may be described by [25]

$$V_P = -P\frac{J_0}{2A}\int_0^l \theta'^2 dz \tag{18}$$

Summarizing, the total potential energy (11) may be presented as

$$V = \frac{1}{2}\int_0^l F(z)dz \tag{19}$$

where the underintegral function is

$$F(z) = E_t J_\omega \theta''^2 + \left(G_t J_d - P\frac{J_0}{A}\right)\theta'^2 + \frac{1}{4}\left(E_t \bar{J}_{00}\theta'^4 + 2E_2 J_{\omega\omega}\theta''^2\right) \tag{20}$$

The necessary condition for the functional extremum (19), well known the Euler–Lagrange [26] equation

$$\frac{d}{dz}\left(\frac{\partial F}{\partial \theta'}\right) - \frac{d^2}{dz^2}\left(\frac{\partial F}{\partial \theta''}\right) = 0 \tag{21}$$

leads to the governing differential equation of the torsional buckling and initial post-buckling of the column

$$E_t J_\omega \theta^{IV} + \left(P\frac{J_0}{A} - G_t J_d\right)\theta'' - \frac{3}{2}E_t \bar{J}_{00}\theta'^2\theta'' + 3E_2 J_{\omega\omega}\left(2\theta''\theta'''^2 + \theta''^2\theta^{IV}\right) = 0 \tag{22}$$

The solution of the non-linear Eq. (22) can be found by means of the perturbation approach, the following expansions up to third power are introduced

$$\theta(z) = \theta_0\theta_1(z) + \theta_0^2\theta_2(z) + \theta_0^3\theta_3(z) + \cdots \tag{23}$$
$$P = P_{cr} + \theta_0 P^{(1)} + \theta_0^2 P^{(2)} + \theta_0^3 P^{(3)} + \cdots$$

where θ_0 stands for a perturbation parameter and P_{cr} denotes the critical buckling load.

Substituting relations (23) into (22) and equating, in accord to the perturbation approach [22], the coefficients of the power of the perturbation parameter to zero the following system of linear differential equations is given

$$E_t J_\omega \theta_1^{IV} + \left(P_{cr}\frac{J_0}{A} - G_t J_d\right)\theta_1'' = 0$$
$$E_t J_\omega \theta_2^{IV} + \left(P_{cr}\frac{J_0}{A} - G_t J_d\right)\theta_2'' = -P^{(1)}\frac{J_0}{A}\theta_1'' \tag{24}$$
$$E_t J_\omega \theta_1^{IV} + \left(P_{cr}\frac{J_0}{A} - G_t J_d\right)\theta_3'' = -\frac{1}{2}P^{(2)}\frac{J_0}{A}\theta_1'' + \cdots$$
$$+ \frac{3}{2}E_t \bar{J}_{00}\theta_1'^2\theta_1'' - 3E_2 J_{\omega\omega}\left(2\theta_1''\theta_1'''^2 + \theta_1''^2\theta_1^{IV}\right)$$

together with the appropriate boundary conditions and additional "false" conditions [22].

3. Critical buckling loads and initial post-buckling behaviour

Consider a simply supported I-column of length l axially compressed by the end loads P presented in Fig. 1. The boundary conditions for both column ends may be written as

$$\theta(0) = \theta''(0) = 0, \theta(l) = \theta''(l) = 0 \tag{25}$$

The additional "false" condition results from an assumption that the perturbation parameter θ_0 is considered the displacement at the mid-span cross-section, thus

$$\theta_1(l/2) = \theta_0, \theta_i(l/2) = 0, i = 2, 3, \ldots \tag{26}$$

The solution of the first differential Eq. (24) accounting for the boundary conditions (25) and (26) leads to the buckling mode and the critical buckling load

$$\theta_1(z) = \theta_0 \sin\frac{\pi z}{l}, \quad P_{cr} = \frac{A}{J_0}\left(\frac{\pi^2}{l^2}E_t J_\omega + G_t J_d\right) \tag{27}$$

Entering these results into the solution of the second Eq. (24) and applying the boundary and "false" conditions we arrive at

$$\theta_2(z) = 0, \quad P^{(1)} = 0 \tag{28}$$

Inserting these results in the third Eq. (24) it reads

$$E_t J_\omega \theta_3^{IV} + \left(P_{cr}\frac{J_0}{A} - G_t J_d\right)\theta_3'' = k_3 \sin\frac{\pi z}{l} + l_3 \sin\frac{3\pi z}{l} \tag{29}$$

where

$$k_3 = \left(\frac{\pi}{l}\right)^2 \left[\frac{J_0}{2A}P^{(2)} - \frac{3}{8}\left(\frac{\pi}{l}\right)^2 E_t\bar{J}_{00} - \frac{3}{4}\left(\frac{\pi}{l}\right)^6 E_2 J_{\omega\omega}\right] \tag{30}$$

$$l_3 = \frac{1}{4}\left(\frac{\pi}{l}\right)^4 \left[-\frac{3}{2}E_t\bar{J}_{00} + 9\left(\frac{\pi}{l}\right)^4 E_2 J_{\omega\omega}\right]$$

The solution of the Eq. (24) can be written as

$$\theta_3 = C_1 + C_2 z + C_3 \sin\frac{\pi z}{l} + C_4 \cos\frac{\pi z}{l} + K_3 \sin\frac{\pi z}{l} + L_3 \sin\frac{3\pi z}{l} \tag{31}$$

The constants C_1, C_2, C_3 and C_4 should be determined from the boundary conditions (25) and additional "false" one (26). Thus we arrive at

$$C_1 = C_2 = C_4 = 0, C_3 = L_3, K_3 = 0, L_3 = \frac{l_3}{72(\frac{\pi}{l})^4} \tag{32}$$

These results lead to the final solution of the Eq. (26) and the second derivative of the axial load with respect to the perturbation parameter $P^{(2)}$

$$\theta_3(z) = \frac{1}{192}\frac{\bar{J}_{00}}{J_\omega}\left[6\left(\frac{\pi}{l}\right)^4 \frac{E_2 J_{\omega\omega}}{E_t\bar{J}_{00}} - 1\right]\left(\sin\frac{3\pi z}{l} + \sin\frac{\pi z}{l}\right) \tag{33}$$

$$P^{(2)} = \frac{3}{4}\left(\frac{\pi}{l}\right)^2 \frac{A}{J_0}E_t\bar{J}_{00}\left[1 + 2\left(\frac{\pi}{l}\right)^4 \frac{E_2 J_{\omega\omega}}{E_t\bar{J}_{00}}\right]$$

The result shown in (28) allows to draw a conclusion that the obtained bifurcation point is symmetrical. Additional stability property of the bifurcation point is determined by $P^{(2)}$ value. If negative, it holds

$$2\left(\frac{\pi}{l}\right)^4 \frac{E_2 J_{\omega\omega}}{E_t\bar{J}_{00}} < -1 \tag{34}$$

here the bifurcation point is unstable, which means that the critical buckling load may be decreased. Thus reduction of the critical load due to inevitable geometric imperfections is possible and the bifurcation point exchange into the limit point [22,25]. Evidently for columns made of linearly elastic material symmetrical and stable bifurcation points [25] occur.

The relative initial post-buckling equilibrium path vs. the rotational angle in the column mid-span can be established by the ratio of the axial load P (23) to the critical buckling load corresponding to the linear model of the column material P_{cr}^l

$$\frac{P}{P_{cr}^l} = \frac{P_{cr}}{P_{cr}^l} + \frac{3}{4}\left(\frac{\pi}{l}\right)^2 \frac{E_t\bar{J}_{00} + 2\left(\frac{\pi}{l}\right)^4 E_2 J_{\omega\omega}}{\left(\frac{\pi}{l}\right)^2 E_t J_\omega + G_t J_d}\theta_0^2 \tag{35}$$

The initial post-buckling equilibrium path may be determined putting first relation (22) and (24) into the first formula (16)

$$\theta(z) = \theta_0 \left\{\sin\frac{\pi z}{l} + \frac{\theta_0^2}{192}\frac{\bar{J}_{00}}{J_\omega}\left[6\left(\frac{\pi}{l}\right)^4 \frac{E_2 J_{\omega\omega}}{E_t\bar{J}_{00}} - 1\right]\left(\sin\frac{3\pi z}{l} + \sin\frac{\pi z}{l}\right)\right\} \tag{36}$$

4. Numerical examples

Numerical examples deal with a simply supported thin-walled I-column made of heat-treated aluminium alloy 6081 (E=68.67 GPa, ν=0.33, σ_0=288 MPa) [19] presented in Fig. 1. Torsional buckling and initial post-buckling behaviour are discussed here. The critical buckling load P_{cr} and the post-buckling equilibrium paths are determined for the non-linear material following the Ramberg–Osgood relation (1) [19] (K=0.002, n=16.16) and compared to load P_{cr}^l corresponding to the linear one. The geometrical characteristics of the I cross-sections necessary to calculate the critical loads and the initial post-buckling path are as follows

$$A = ht_h + 2bt_b$$

$$J_0 = \frac{h^3 t_h}{12}\left[1 + 6\frac{b}{h}\frac{t_b}{t_h} + 2\left(\frac{b}{h}\right)^3 \frac{t_b}{t_h}\right]$$

$$J_{00} = \frac{h^5 t_h}{80}\left\{1 + 2\left(\frac{t_b}{t_h}\right)\left[\left(\frac{b}{h}\right)^5 + \frac{5}{12}\left(\frac{b}{h}\right)^3 + 5\frac{b}{h}\right]\right\} \tag{37}$$

$$J_\omega = \frac{1}{24}b^3 h^2 t_b$$

$$J_{\omega\omega} = \frac{1}{640}b^5 h^4 t_b$$

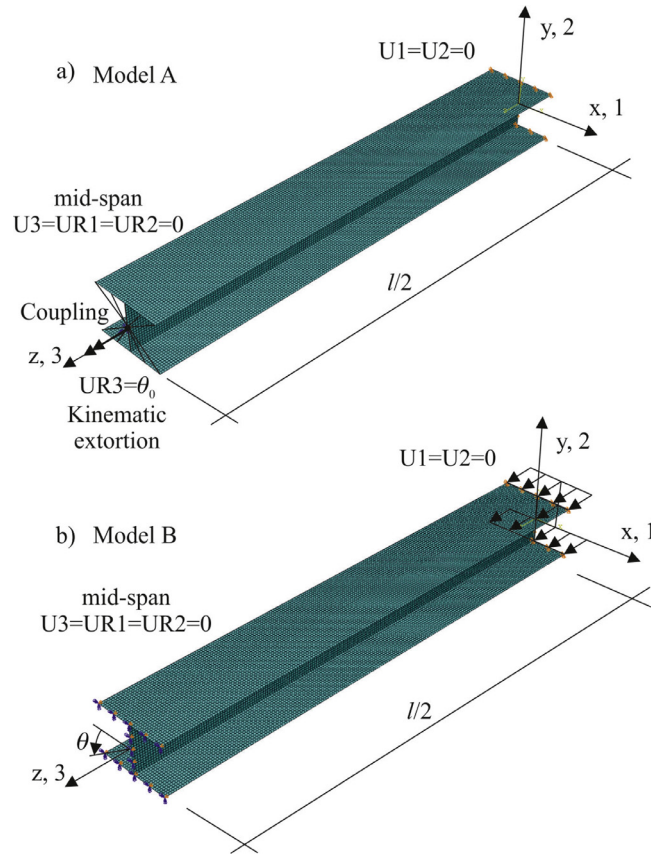$$J_d = \frac{ht_h^3}{3}\left[1 + 2\left(\frac{t_b}{t_h}\right)^3 \frac{b}{h}\right]$$

Fig. 2. Three-dimensional FE models, boundary conditions and load diagrams: (a) Model A, (b) Model B.

Table 1
Axially compressed simply supported column – critical buckling force (kN).

l (m)	t_b (mm)	P_0 (5)	Analytic		Diff.	FEM		Diffs.		
			Linear (3)	R–O (4)	(%)	Linear (LBA)	R–O (Riks)	(%)	(%)	(%)
3.5	5	2016	*1955.3*	**1582.9**	19.0	*1916.9*	**1605.8**	16.2	*2.0*	**1.4**
	10	2304	*2275.5*	**1817.7**	20.1	*2229.2*	**1851.4**	16.9	*2.0*	**1.8**
4	5	2016	*1578.4*	**1464.2**	7.2	*1562.5*	**1477.3**	5.5	*1.0*	**0.9**
	10	2304	*1857.7*	**1696.6**	8.7	*1830.3*	**1713.9**	6.4	*1.5*	**1.0**

The analytical solutions are verified by means of the results of FEM analysis. Numerical analysis is performed by means of the ABAQUS software [24]. In order to estimate values of the critical buckling loads the linear (Linear Buckling Analysis) and non-linear (Riks) [27–29] procedures are applied. In the numerical analysis by ABAQUS software the non-linear behaviour of material (aluminium alloy 6081) is described by two parameters of the Ramberg–Osgood law (ABAQUS – Material Behaviours – Mechanical – Deformation Plasticity): the "yield" offset $\alpha = K \frac{E}{\sigma_0} = 0.476875$ and the hardening exponent $N = n-1 = 15.16$. In the FEM analysis, due to symmetry of the member, only a half of the column was discretised with boundary conditions presented in Fig. 2. In all numerical analysis the members are modelled by means of fully integrated shell elements with a reduced integration type S4R. The main finite element size is 0.01×0.01 m^2 (i.e. 80 elements are used along the cross-sections and for: $l/2 = 1.75$ m − 175; $l/2 = 2$ m − 200 along the length of the member). The total amount of finite elements applied is: $l/2 = 1.75$ m − 14,000 and $l/2 = 2$ m − 16,000. Prior to numerical stability analysis of the problem convergence of the applied FEM procedure is investigated. In Fig. 2 numerical models, FEM mesh, load and imposed boundary conditions are shown. The numerical calculations were performed by means of two models (Fig. 2): first (a) Model A to find a starting non-perfect geometry using kinematic extortion θ_0 (10^{-5} or 20^{-5} rad) and *COUPLING constraints command (see Fig. 2a) (using *STATIC, GENERAL command) and next (b) Model B (see Fig. 2b) used in the main analysis (using *STATIC, RIKS command) with initial imperfections taken from Model A (using *IMPERFECTION command).
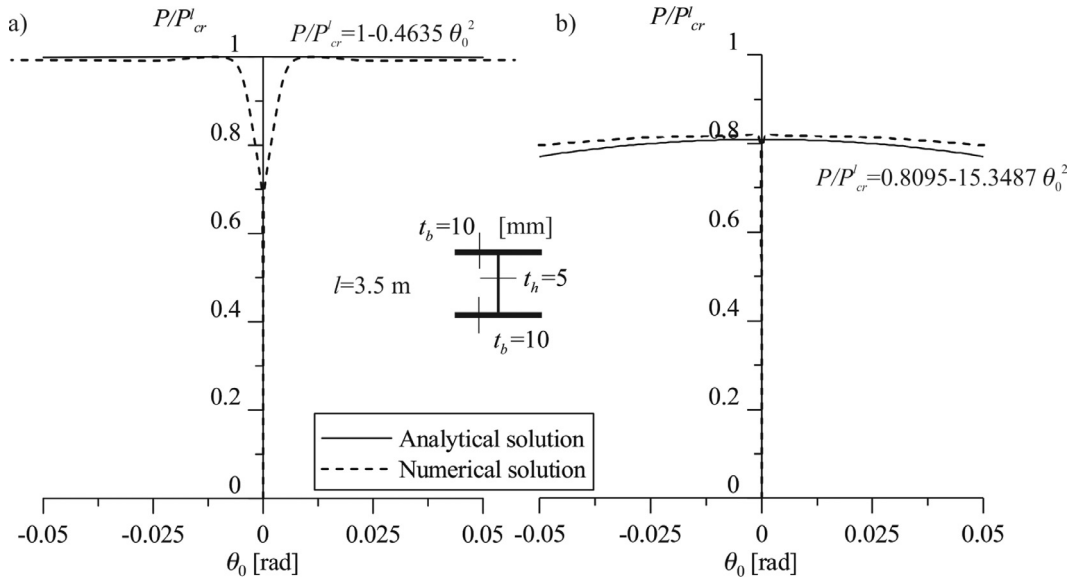
Fig. 3. Relative critical torsional buckling load vs. middle-span deflection for simply supported column; length 3.5 m and web thickness $t_h=5$ mm for (a) linear and (b) non-linear material.
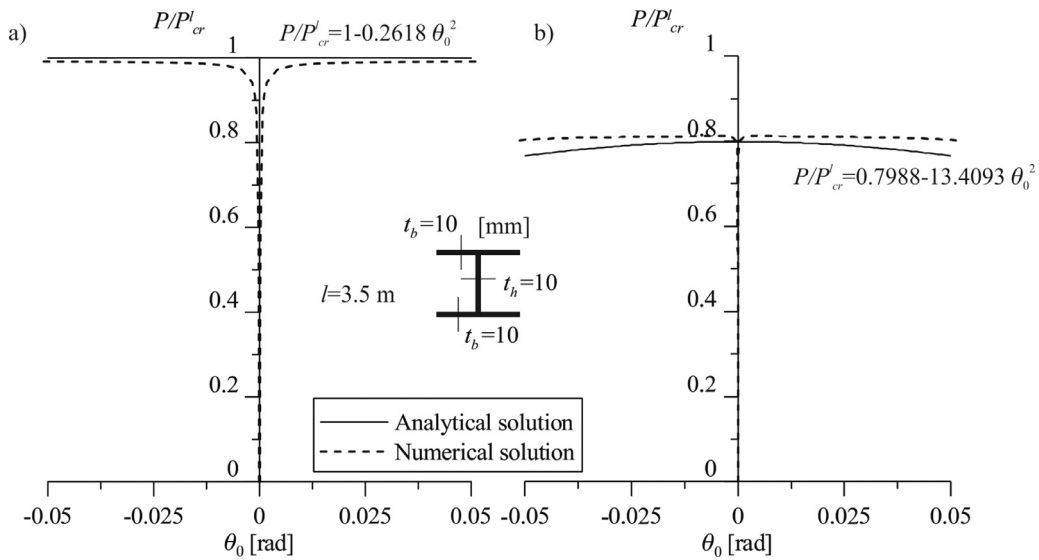

Fig. 4. Relative critical torsional buckling load vs. middle-span deflection for simply supported column; length 3.5 m and web thickness $t_h=10$ mm for (a) linear and (b) non-linear material.

Tables 1 and Figs. 3–6 presents the critical buckling loads and the relations of the critical load to the one corresponding to linearly elastic material vs. the rotation at mid-span cross-section.

The slenderness ratios λ for the analysed cross-sections were investigated. If $l=3.5$ m the λ equals 43.6 at $t_h=5$ mm and 46.6 at $t_h=10$ mm and if $l=4$ m λ equals 49.9 at $t_h=5$ mm and 53.3 at $t_h=10$ mm. In all cases the slenderness ratios λ are higher than the reference slenderness ratio $\lambda_r = \pi\sqrt{\frac{E}{\sigma_0}}=15.4$.

Moreover the initial post-buckling equilibrium paths are shown in Figs. 7 and 8. Additionally in the Table 1 the values of limit forces P_0 are shown. Comparison of the results obtained allows to draw a conclusion that analytical and numerical solutions converge.
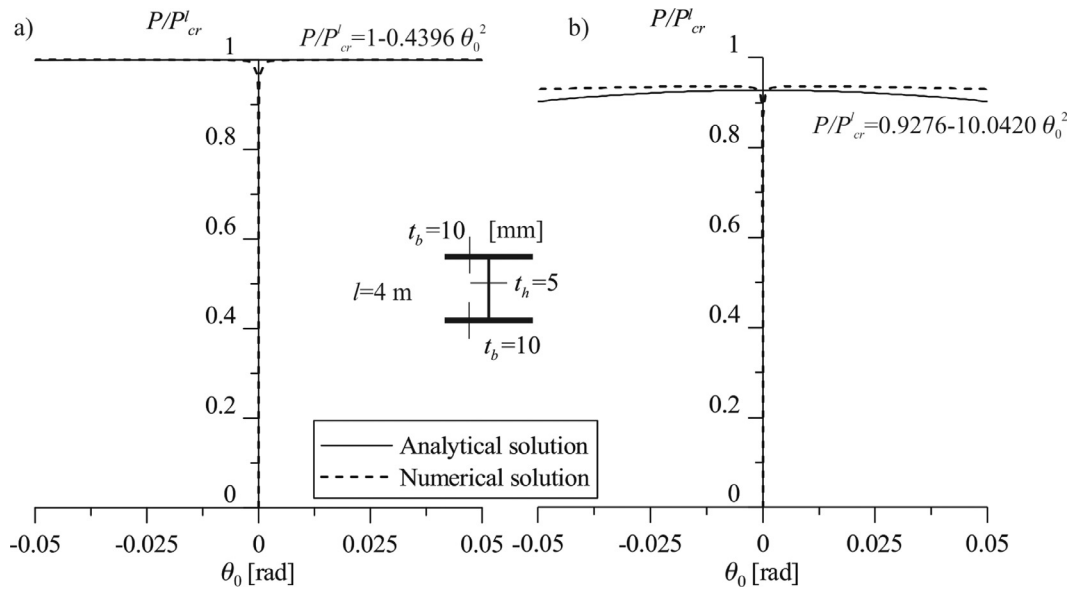
Fig. 5. Relative critical torsional buckling load vs. middle-span deflection for simply supported column; length 4 m and web thickness t_h=5 mm for (a) linear and (b) non-linear material.

Fig. 6. Relative critical torsional buckling load vs. middle-span deflection for simply supported column; length 4 m and web thickness t_h=1 mm for (a) linear and (b) non-linear material.
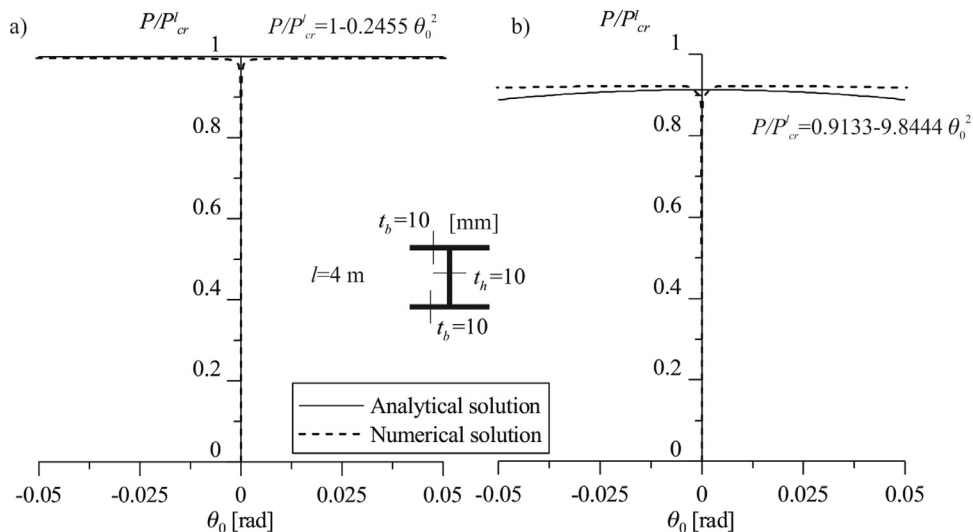
5. Discussion and conclusions

Torsional buckling and initial post-buckling behaviour of the axially compressed columns with bisymmetrical cross-section made of aluminium alloy are considered. Closed analytical formulas for the torsional critical buckling load and post-buckling behaviour are stated. Additionally, the initial post-buckling equilibrium path is derived. It should be noted that the Ramberg–Osgood constitutive equation may be also applied for other materials, for example: stainless-steel, carbon-steel or wood and in these cases it is possible to use the method of stability analysis presented herein. Finally, the comparative numerical analysis using the commercial computer system ABAQUS is carried out.

The analytical and numerical study allows to formulate some conclusions related to effect of material non-linearity on the torsion critical load and initial post-buckling behaviour. The results of the FEM analysis confirm correctness of the proposed analytical solutions and their acceptable accuracy. The small discrepancies observed may be a result from neglecting the cross-section deformability in the analytical solution.
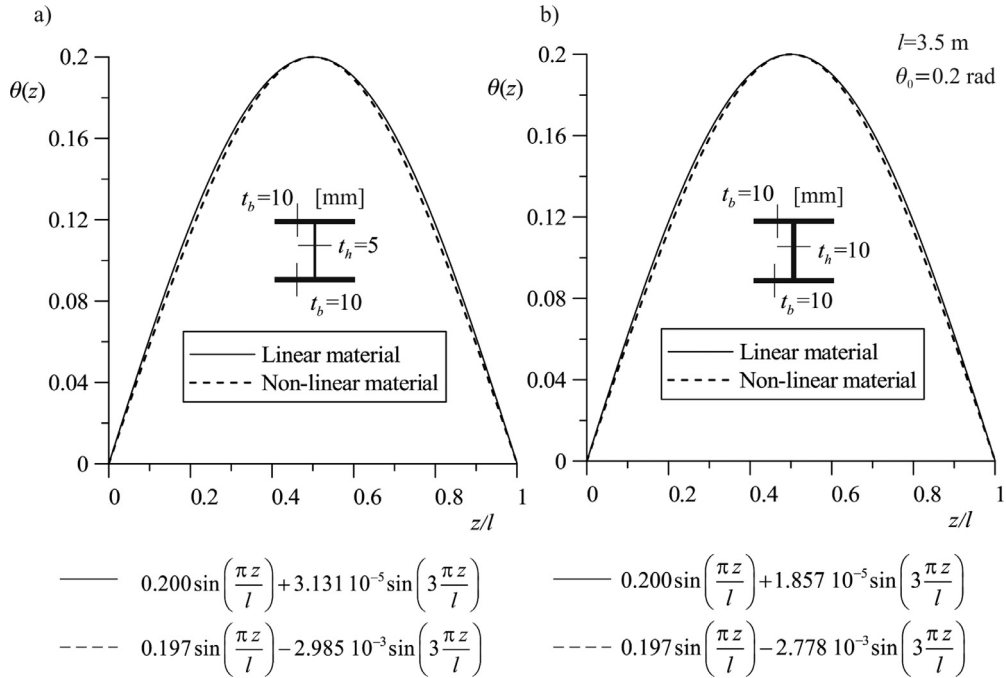
a)

b)

$$l=3.5\text{ m}$$
$$\theta_0=0.2\text{ rad}$$

——— $0.200\sin\left(\dfrac{\pi z}{l}\right)+3.131\ 10^{-5}\sin\left(3\dfrac{\pi z}{l}\right)$

- - - - $0.197\sin\left(\dfrac{\pi z}{l}\right)-2.985\ 10^{-3}\sin\left(3\dfrac{\pi z}{l}\right)$

——— $0.200\sin\left(\dfrac{\pi z}{l}\right)+1.857\ 10^{-5}\sin\left(3\dfrac{\pi z}{l}\right)$

- - - - $0.197\sin\left(\dfrac{\pi z}{l}\right)-2.778\ 10^{-3}\sin\left(3\dfrac{\pi z}{l}\right)$

Fig. 7. Relative initial post-buckling equilibrium path for simply supported column; length 3.5 m and web thickness: (a) $t_h=5$ mm and (b) $t_h=10$ mm for linear and non-linear material – analytical results.

a)

b)

$$l=4\text{ m}$$
$$\theta_0=0.2\text{ rad}$$

——— $0.200\sin\left(\dfrac{\pi z}{l}\right)+3.131\ 10^{-5}\sin\left(3\dfrac{\pi z}{l}\right)$

- - - - $0.197\sin\left(\dfrac{\pi z}{l}\right)-2.020\ 10^{-3}\sin\left(3\dfrac{\pi z}{l}\right)$

——— $0.200\sin\left(\dfrac{\pi z}{l}\right)+1.857\ 10^{-5}\sin\left(3\dfrac{\pi z}{l}\right)$

- - - - $0.197\sin\left(\dfrac{\pi z}{l}\right)-2.159\ 10^{-3}\sin\left(3\dfrac{\pi z}{l}\right)$
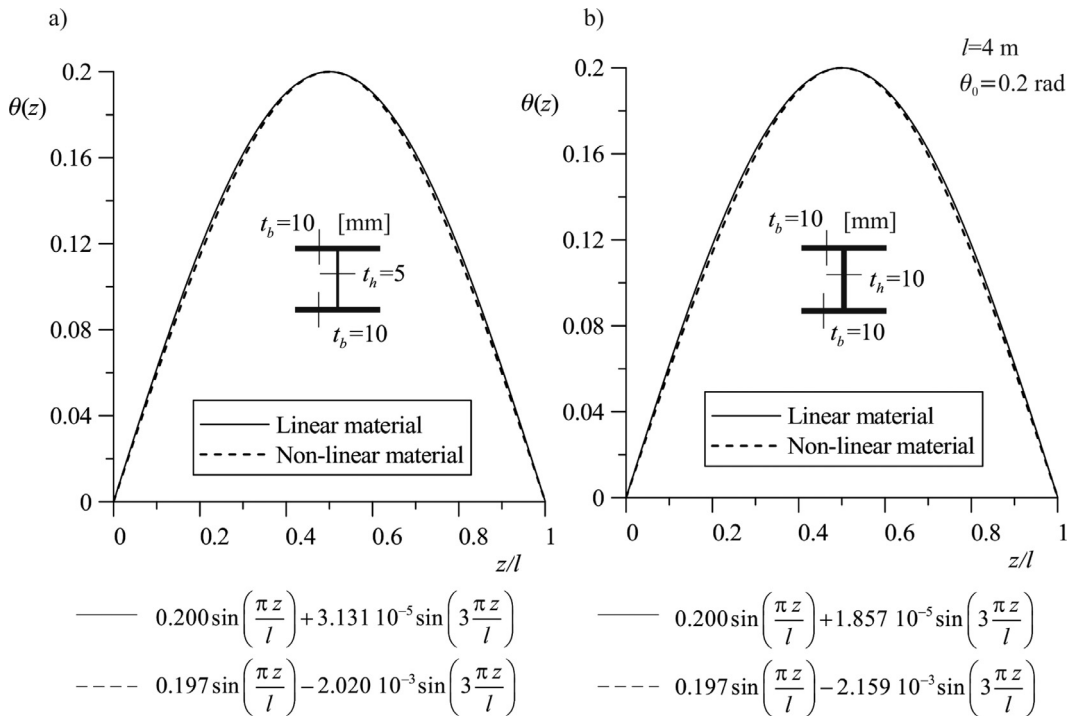
Fig. 8. Relative initial post-buckling equilibrium path for simply supported column; length 4 m and web thickness: (a) $t_h=5$ mm and (b) $t_h=10$ mm for linear and non-linear material – analytical results.

It should be noticed that the sign of the reduced fourth order polar moment of inertia $\bar{J}_{00}$ value defines the type of bifurcation point in an elastic range of the column material behaviour. If the polar moment of inertia $\bar{J}_{00}$ is positive, a symmetric and stable bifurcation point exists and the reduction of critical load due to geometrical imperfections does not occur. In the case of the negative value of $\bar{J}_{00}$, the bifurcation point is unstable and such a reduction occurs (see Figs. 3(a), 4(a), 5(a), 6(a)). Otherwise it is noteworthy that the bifurcation point of flexural buckling is symmetric and stable in the elastic range of the material behaviour. In the case of material non-linearity, in view of the negative dominate value of E_2 module (9) and (10), the bifurcation point is usually symmetric but unstable and causes decrement of the critical buckling load.

A higher reduction of the critical buckling stress occurs if its value is close to the elastic limit. It is also noteworthy that, the case happens only for heat-treated aluminium alloys [19]. In the case of non-heat-treated aluminium alloys [19] prior to loss of the torsional of stability the material usually becomes plastic. This phenomenon is very important aluminium structural design constructions in order to fulfill stability and stress conditions.

References

[1] F.M. Mazzolani, Aluminium Alloy Structures, E&FN Spon, 1995.
[2] J.R. Kissell, R.L. Ferry, Aluminum Structures, a Guide to Their Specifications and Design, John Wiley and Sons, Inc., 2002.
[3] F.M. Mazzolani, Aluminum Structural Design, no. 442, Springer-Verlag Wien GmbH, 2003.
[4] N.S. Trahair, Flexural-Torsional Buckling of Structure, 1st ed., E&FN Spon, 1993.
[5] L. Valarinho, J.R. Correia, M. Machado-e Costa, F.A. Branco, N. Silvestre, Lateral-torsional buckling behaviour of long-span laminated glass beams: analytical, experimental and numerical study, Mater. Des. 102 (2016) 264–275.
[6] P. Jiao, W. Borchani, S. Soleimani, B. McGraw, Lateral-torsional buckling analysis of wood composite I-beams with sinusoidal corrugated web, Thin-Walled Struct. 119 (2017) 72–82.
[7] X. Guo, Z. Xiong, Z. Shen, Flexural-torsional buckling behavior of aluminum alloy beams, Front. Struct. Civ. Eng. 9 (2) (2015) 163–175.
[8] Y.Q. Wang, H.X. Yuan, Y.J. Shi, M. Cheng, Lateral-torsional buckling resistance of aluminium I-beams, Thin-Walled Struct. 50 (2012) 24–36.
[9] B. Yanga, S. Kanga, G. Xionga, S. Niea, Y. Hua, S. Wanga, J. Baia, G. Daia, Experimental and numerical study on lateral-torsional buckling of singly symmetric Q460GJ steel i-shaped beams, Thin-Walled Struct. 113 (2017) 205–216.
[10] J. Belis, C. Bedon, C. Louter, C. Amadio, R.V. Impe, Experimental and analytical assessment of lateral torsional buckling of laminated glass beams, Eng. Struct. 51 (2013) 295–305.
[11] O. Pešeka, J. Melcher, Lateral-torsional buckling of laminated structural glass beams, Procedia Eng. 190 (2017) 70–77.
[12] G. Piana, E. Lofrano, A. Manuello, G. Ruta, A. Carpinteri, Compressive buckling for symmetric TWB with non-zero warping stiffness, Eng. Struct. 135 (2017) 246–258.
[13] C.K. Rao, L.B. Rao, Torsional post-buckling of thin-walled open section clamped beam supported on Winkler–Pasternak foundation, Thin-Walled Struct. 116 (2017) 320–325.
[14] D.G. Ninh, D.H. Bich, B.H. Kien, Torsional buckling and post-buckling behavior of eccentrically stiffened functionally graded toroidal shell segments surrounded by an elastic medium, Acta Mech. 226 (2015) 3501–3519.
[15] D.V. Dung, L.K. Hoa, Research on nonlinear torsional buckling and post-buckling of eccentrically stiffened functionally graded thin circular cylindrical shells, Compos. Part B 51 (2013) 300–309.
[16] S.S. Antman, Non-linear problems of elasticity, Applied Mathematic Science, Vol. 107, 2nd ed., Springer, 2005.
[17] G.J. Hancock, Cold-formed steel structures: research review 2013–2014, Adv. Struct. Eng. 19 (3) (2016) 393–408.
[18] G.J. Hancock, Cold-formed steel structures, J. Constr. Steel Res. 59 (2003) 473–487.
[19] K.J.R. Rasmussen, J. Ronald, Strength curves for aluminium alloy columns, Eng. Struct. 23 (2000) 1505–1517.
[20] D. Wei, M.B.M. Elgindi, Finite element analysis of the Ramberg–Osgood bar, Am. J. Comput. Math. 3 (2013) 211–216.
[21] W. Ramberg, W. Osgood, Description of stress–strain curves by tree parameters, Technical Report, National Advisory Committee for Aeronautics, 1943.
[22] J.M.T. Thompson, G.W. Hun, A General Theory of Elastic Stability, John Wiley & Sons, 1973.
[23] O. Basquin, Tangent modulus and the strength of steel columns in test, Technical Report, Department of Commerce, Bureau of Standards USA, 1924.
[24] D. Habbit, B. Karlsson, P. Sorensen, ABAQUS Analysis User's Manual, Hibbit, Karlsson, Sorensen Inc.,
[25] C. Szymczak, Buckling and initial post-buckling behaviour of thin walled I-columns, Comput. Struct. 11 (1980) 481–487.
[26] I.M. Gelfand, S.V. Fomin, Calculus of Variations, Prentice-Hall, Englewood Cliffs, New York, 1963.
[27] M. Crisfield, A fast incremental/iterative solution procedure that handles snap through, Comput. Struct. 13 (1981) 55–62.
[28] E. Ramm, Nonlinear Finite Element Analysis in Structural Mechanics, Springer-Verlag, 1981.
[29] G. Powell, J. Simons, Improved iterative strategy for nonlinear structures, Int. J. Numer. Methods Eng. 17 (1981) 1455–1467.